1. Introduction

1.1. Motivation

Wireless communication technology showed a fast growth rate during the past decades. Starting from the 1980s, research efforts have been devoted to the development of wireless communication systems. Fig. 1.1 shows the evolution of wireless communication system. While the key performance indices are predicted values, the 6G white paper recently published recommends 140 GHz as the system frequency with a peak data rate of 100 Gbps to 1 Tbps. Applications using wireless communication technology such as the End-to-End architecture shown in Fig. 1.2 were increasing rapidly during the past years. Obviously, the requirement of data rate for each generation of the communication system has increased severely with the thriving of innovative applications. For instance, mobile applications in fourth-generation Long-Term-Evolution (4G LTE) networks and smart city targeted for the fifth-generation (5G) communication system. These data-hungry applications are the driving forces for the tremendous evolution of wireless communication systems which proceeds in ever shorter evolution cycles.

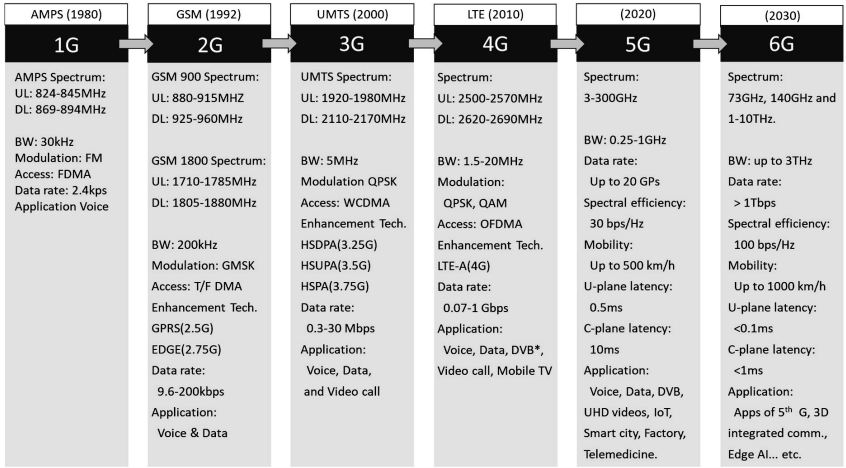

Figure 1.1. Evolution of wireless communication system [1].

Fig. 1.3 shows the timeline of wireless communication systems. A duration of 15 years from standardizing the specification to deployment has been taken for the third-generation (3G) communication system; as for 4G, the duration was 12 years. For the ongoing 5G communication system, an estimation of 8 years from standardizing to full deployment has been made. Communication system technology beyond 5G is expected to have even shorter duration as shown in the figure. While targeting for a higher data transmission rate, the available spectrum for the implementation of communication systems seems to be a critical issue. This

is mainly attributed to a crowded spectrum at sub-6 GHz frequencies with a variety of commercial applications. To seek for higher spectral efficiency, moving up to millimeter-wave frequencies is considered as a potential solution.

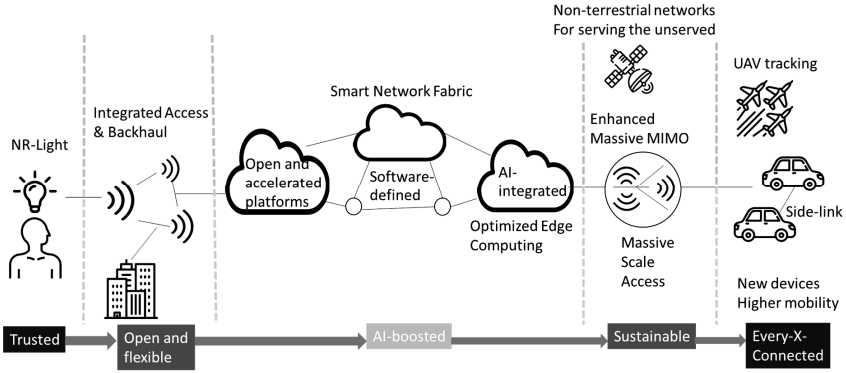

Figure 1.2. End-to-End (E2E) architecture [2].

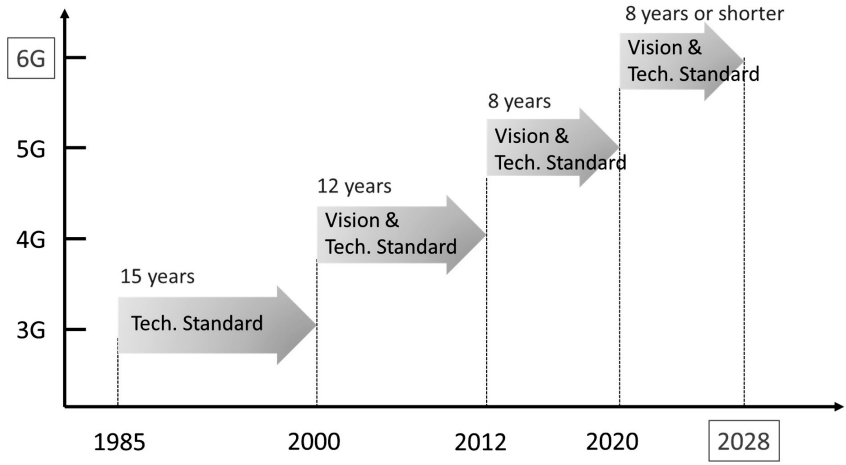

Figure 1.3. Timeline of wireless communication systems [3].

Referring to the Shannon-Hartley theorem [4], a wider operating bandwidth and high signal-to-noise ratio (SNR) are required for the realization of high capacity 5G wireless network. The peak data rate and capacity of a radio channel can be expressed as:

$$\text{Peak data rate of a radio channel} = BW \cdot n \cdot M \tag{1.1}$$

$$\text{Capacity of a radio channel} = BW \cdot n \cdot \log_2\left(1 + SNR\right) \tag{1.2}$$

Note that BW stands for bandwidth, n stands for the number of spatially separated paths and M represents the number of bits. The two equations highlight the importance of channel bandwidth for enhancing performance of communication system. Fig. 1.4 shows the frequency allocation for 5G communication systems over the world.

As shown in Fig. 1.1, 5G communication system serves a higher bandwidth and lower latency comparing with the existing 4G communication system. Fig. 1.3 shows that the 5G spectrum allocation around the world have been majorly focusing at Ka-band frequencies in vicinity of 28 and 38 GHz. The European Telecommunications Standards Institute (ETSI) has announced the 5G New Radio (NR) frequency range 2 (FR2) [6], where five channels are defined as 26.5 – 29.5 GHz (n257), 24.25 – 27.5 GHz (n258), 39.5 – 43.5 GHz (n259), 37 – 40 GHz (n260) and 27.5 – 28.35 GHz (n261).

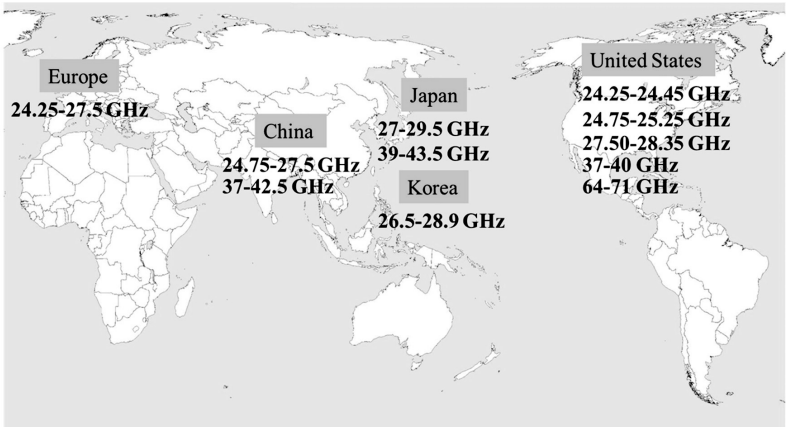

Figure 1.4. Global viewgraph of allocated 5G spectrum [5].

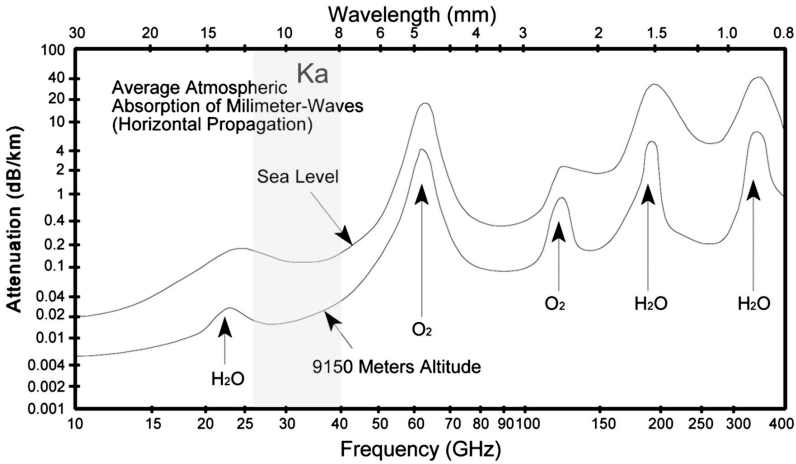

Figure 1.5. Average atmospheric attenuation at millimeter-wave frequencies [10].

For millimeter-wave applications, it can be expected that high attenuations such as atmospheric loss [7], dielectric loss in substrates [8] and metallic loss in conductors [9] severely influence amplifier efficiencies. Such drawbacks have led to the difficulties in the deployment of the basic infrastructure. Fig. 1.5 shows the average atmospheric absorption at millimeter-wave frequencies from 10 GHz up to 400 GHz, where Ka-band frequencies are marked in light blue.

To overcome the high attenuation at millimeter-wave frequencies, enhancement in the overall performance of the communication system in terms of gain and output power are considered as a critical issue. However, the severe degradation of maximum available device gain (MAG) as shown in Fig. 1.6 at high operating frequencies makes it difficult to meet system specifications. To further increase the MAG at higher operating frequency, scaling down the gate length of devices in conjunction with a systematic reduction of parasitic capacitive, inductive and ohmic losses in the devices are considered as straightforward methods. Fig. 1.7 shows the status of popular device technologies implemented for millimeter-wave and submillimeter-wave circuits. Although the maximum operating frequency has been pushed to a very high level, the shorter gate length is expected to limit the breakdown voltage of the devices. The output power can be expressed as:

$$P_{out} = \frac{\left(I_{D,\max} - I_{D,\min}\right) \times \left(V_{D,\max} - V_{D,\min}\right)}{8} \tag{1.3}$$

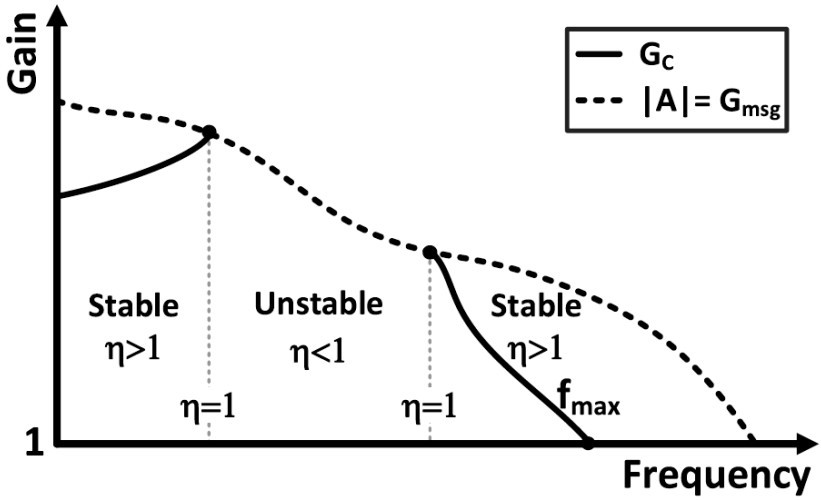

Figure 1.6. Maximum available gain and maximum stable gain as an interval of frequency [11].

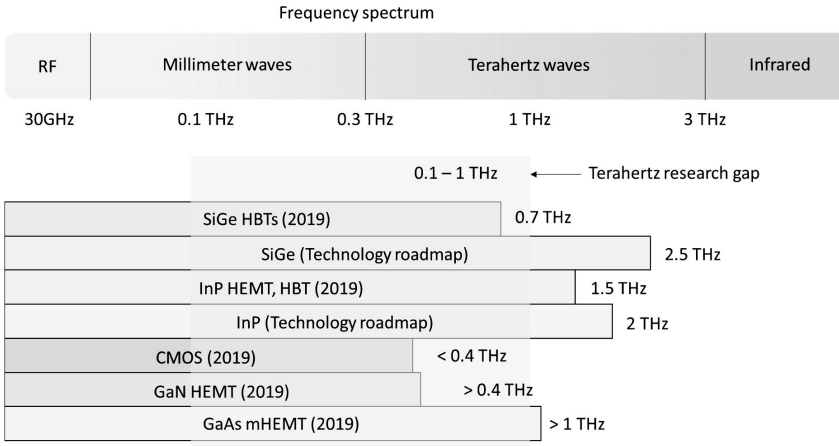

Figure 1.7. Maximum operating frequency of different device technologies [12].

Therefore, the breakdown voltage of the device may limit the maximum drain voltage allowed for the proper operation. According to eq.1.3 this also limits the maximum output power of the device. To seek for higher output power density at higher frequencies, compound semiconductor device technologies with relatively high breakdown voltage characteristics are considered as ideal candidates for applications at millimeter-wave frequencies and beyond. Fig. 1.8 plots the saturated output power (P_{sat}) of amplifiers as a function of frequency in log scale using different device technologies. Focusing at the frequency range between 10 to 100 GHz,

device technologies with higher breakdown voltage such as gallium arsenide (GaAs) and gallium nitride (GaN) are showing outstanding performance in terms of output power at millimeter-wave frequencies comparing with CMOS technologies. As for indium phosphide (InP), it is showing a nice performance for applications beyond 300 GHz. Regarding the trend for GaN-based amplifiers, the P_{sat} of the reported power amplifiers at frequency above W-band drops severely. Comparing with mature III-V technologies including GaAs and InP, GaN technologies are still under development for operating frequencies beyond W-band. For recent publications, GaN-based power amplifiers beyond W-band frequencies were majorly focusing on the gain improvement instead of output power. This was mainly due to the relatively low frequency response characteristics comparing with GaAs and InP technologies, leading to a lower MAG level. The output power level was not a big issue for GaN-based amplifiers as it was stated that the high breakdown voltage allowed a higher voltage supply at the drain node, which resulted in a greater output power density. Therefore, it can be inferred that the slope of the trend can be smoothed soon in the future with the improvement of frequency response and device structure optimization.

Although each of the device technology has its shortage while pushing the limits of maximum operating frequency, systematical design methods have been widely reported for circuitries at high frequencies [14]-[17].

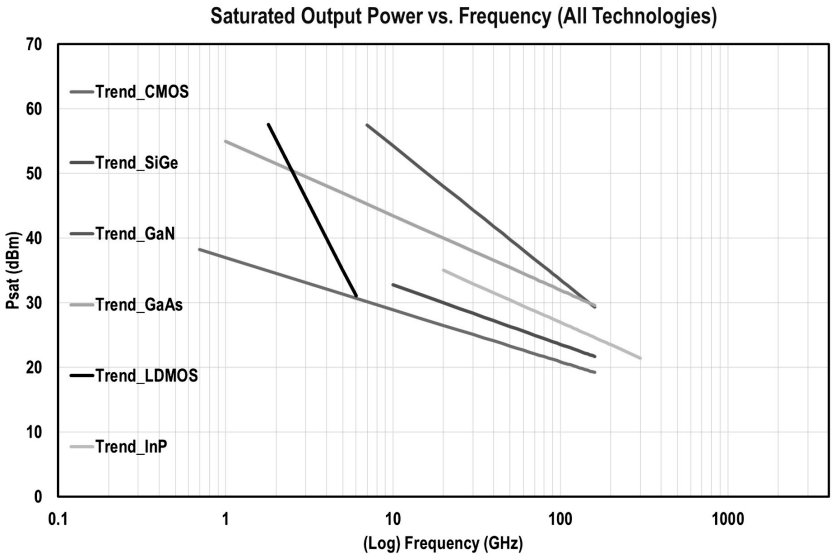

Figure 1.8. Saturated output power of amplifiers as a function of frequency using different device technologies [13].

To push boost up the deployment of 5G communication system, design technologies taking care of the specific requirements dictated by the semiconductor technologies applied have to be

taken into account. Hence, transceivers with high gain, high power for overcoming the atmospheric attenuation are necessary to support the operation at commercial bands regulated for 5G NR FR2.

1.2. Requirements for beam steering mm-wave transceivers

For millimeter-wave applications, the propagation characteristics affecting the transmitting and receiving of transceivers have been discussed in the previous section. Based on the discussion, the first issue to solve will be the free space path loss (L_{fsl}), which is expressed as [18]:

$$L_{fsl} = 32.44 + 20\log f + 20\log R - \mathrm{G_{Tx}} - G_{\mathrm{Rx}} \tag{1.3}$$

Note that f represents frequency in GHz, R is the distance between antennas in m, $\mathrm{G_{Tx}}$ and $\mathrm{G_{Rx}}$ are the overall transmitter/receiver antenna gain including feeding loss. For long distance transmission, the free path loss is considered as an extreme challenge for evaluating the link budget for the transceiver system. To overcome the issue, antennas with high gain and high directivity are promising candidates to solve the issue. However, the atmospheric attenuation is not the only application concern for transceiver at millimeter-wave frequencies. Obstacles such as walls and other objects are known to induce high penetrating losses at millimeter-wave frequencies [19]. Therefore, plenty of issues regarding the induced losses must be carefully considered prior to the design of the transceiver system. Beam steerable antennas have caught researchers' eyes as the ability of reconfiguring radiation patterns to maintain proper signal transmission in the network.

Beam steering antennas were first implemented at low frequencies for systems requiring high directivity beams to prevent unwanted signals. Take a receiver with omnidirectional radiation pattern as an example, the signals from each device may cause interference with each other while receiving the signal of interest. To properly receive the desired signal without the interference of unwanted signals, the beam steering antennas are able to reconfigure the propagation beam in such a way that the transmission of the desired signal approaches an optimum. Such arrangements improve system performance as the interference has been reduced. Fig. 1.9 shows the diagram for illustration of beam steering with multiple devices.

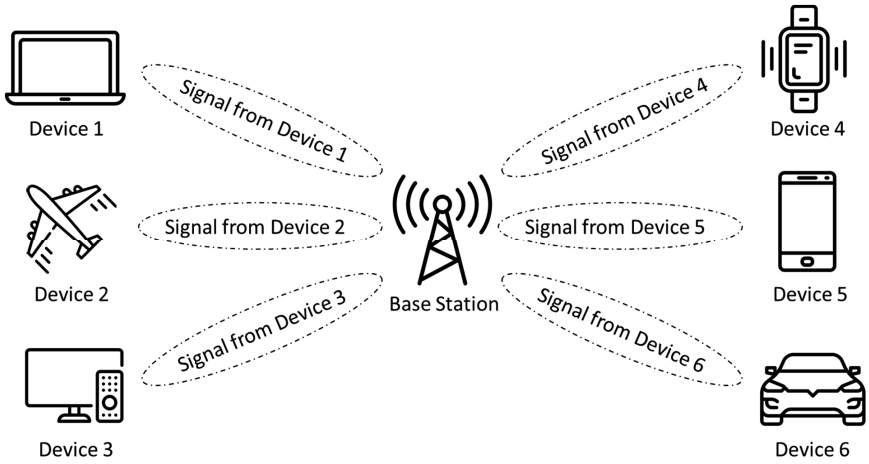

Figure 1.9. Illustration of beam steering approach.

Beam steering technique has some important properties to maintain for operation:

1. When an object is presenting the transmitting path, an additional insertion loss is induced and degrades the transmission of power delivered to the system.

2. The steering range of a beam steering antenna system is another concern for design. It depends on particular design and implementation of the individual antennas and of the phase shifter network. For example, a horn antenna using non-uniform flexible meta-surface allows for a steering range of the main beam of 80^{o} as reported in [20].

3. The steering resolution (S-Res) of the beam steering antenna system can be set as continuous, predefined or finite. The setting will affect the increment of the steering range, which mainly depends on the needed steering angle for the system.

4. The sensitivity of the beam steering system will be determined by the steering speed. However, this depends on the environment for operation.

Table 1.1 presents an overview of the beam steering techniques [21]-[30]. A variety of research utilizing different beam steering techniques have been published in conferences or journals, showing a nice performance at millimeter-wave frequencies.

Table 1.1. Comparison table for common beam steering techniques.

Technique	IL	S-Res	Complexity	Size	Cost
TWA	None	Continuous	Low	Small	Low
ILAs	Low	Predefined	Low	Medium	Low
Parasitic	Low	Predefined	Low	Depending	Low
Mechanical	None	Continuous	Low	Large	Low

Digital BF	High	Fine	High	N/A	High
Analog BF	High	Predefined	Moderate	Medium	High
Reflect Array	Medium	Predefined	Moderate	Large	High
SBA	Medium	Predefined	Low	Large	High
R-Arrays	Low	Fine	Moderate	Medium	Medium
Metamaterial	High	Predefined	Moderate	Medium	Medium

Traveling wave antenna (TWA); Integrated lens antenna (ILA); Parasitic steering; Beamforming (BF); Switched beam antennas (SBA); Reflect arrays (R-Arrays)

1.3. State-of-the-Art in transceiver technology

With the deployment of 5G communication systems, applications are expanding their operating frequency into millimeter-wave region. For high speed data links, phased-array transceivers composed of multiple antenna arrays and RF front-ends are adopted to achieve high equivalent isotropic radiated power (EIRP). Such arrangement with phased-arrays enables multiple applications such as high speed link connecting base station interacting with mobile devices [19], [31]. The 5G commercial spectrum has launched sub-6 GHz systems at the early stage. The combination with already existing 4G communication systems initially reduced complexity. To push the operating frequency up to Ka-band frequencies and beyond, it is necessary for the antenna system to support a large number of controllable beams using cost-efficient arrangements suitable for realistic deployment. In this connection, Global Foundries developed a circuit block of 32 TRx module including RF phase shifting, switched TRx and simultaneous H/V polarization architectures based on their 8HP 130-nm SiGe BiCMOS process. Fig. 1.10 [32] shows the block diagram of this particular module. For the switched TRx, antenna switches controlling the signal path, low-noise amplifier improving Rx sensitivity and power amplifier improving the EIRP of Tx with nice linearity are designed and integrated in a single chip. As for the RF phase shifting architecture, the available phase control range enables beamforming operation, nice phase shifting resolution is required for improving side-lobe suppression to minimize the phase error induced while beam steering. A variable gain amplifier (VGA) was designed to expand the control range of RF gain, which enables a high level side-lobe rejection and minimize the complexity of system calibration.

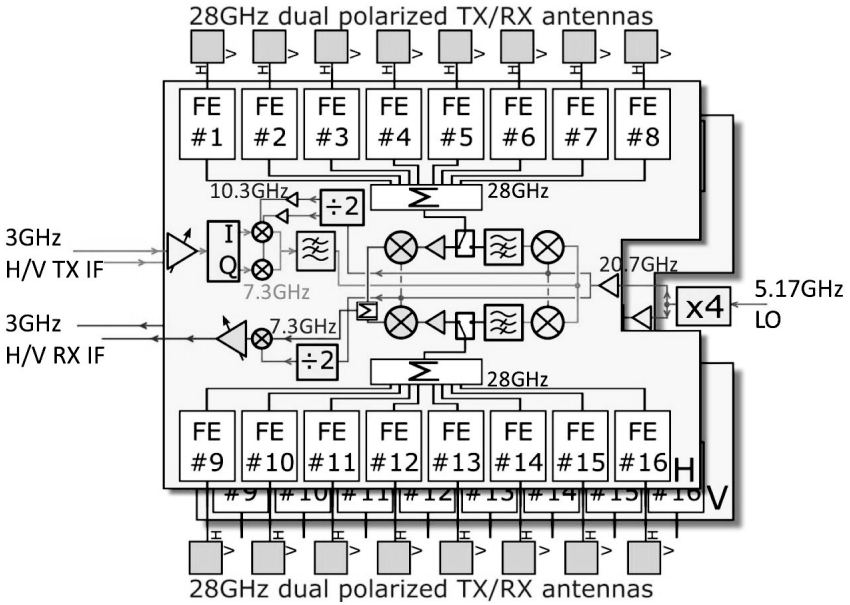

Figure 1.10. Schematic for the building block of TRx module [32].

For the single chip solution, characterization of the transceiver must go through three stages including on-wafer measurements, packaged IC for over the air tests and connectorized package to be wired with a millimeter-wave interface to process further characterizations. The antenna-in-package (AiP) approach has been widely reported in CMOS and SiGe technologies for millimeter-wave applications [32]-[35].

As for antenna on printed-circuit-board (PCB) approaches [36]-[39], it often required a large number of chips for further integration. However, there are several disadvantages for the antenna on PCB approach. For instance, large propagation loss degrading the transmitted power while scaling up the number of arrays. In [39], the 2 × 2 TRx beamformer chips with symmetric design using Wilkinson power divider/combiner was proposed for overcoming the disadvantage of antenna on PCB approaches. Fig. 1.11 shows the building block of the N × N phased-array with 2 × 2 TRx beamformer on PCB. To improve the transmitted power and noise figure of the system, the routing distance between the chip and antenna feeds was minimized for reduction of the conversion loss. The scalable characteristic by using symmetry Wilkinson networks can modify the dimension of the module based on the system specifications. With a large number of elements to be implemented in the phased-array system, heat dissipation induced by the chips are considered as a critical issue as this may have led to degradation of the overall performance. To overcome such issue, apertures have designed on the PCB to spread out the heat without disturbing antenna efficiency. Silver paint with a thermal conductivity of 9.1 W/m·K and low sheet resistance of 0.08 Ω/□·μm was applied to connect the front and backside of the PCB. Such arrangement helped to maintain the available transmitted power for